Vol 15 No 3, March 2006
1009-1963/2006/15(03)/0593-07

Chinese Physics

© 2006 Chin. Phys. Soc.
and IOP Publishing Ltd

Tomographic analysis of the central magnetohydrodynamic oscillations on the HT-7 tokamak*

Ma Tian-Peng(马天鹏)[a)†], Ruan Huai-Lin(阮怀林)[b)], Hu Li-Qun(胡立群)[a)], Wan Bao-Nian(万宝年)[a)], Gao Xiang(高 翔)[a)], Zhen Xiang-Jun(甄香君)[a)], Zhou Li-Wu(周立武)[a)], Sun You-Wen(孙有文)[a)], Gao Wei(高 伟)[a)], Chen Zhong-Yong(陈忠勇)[a)], Lin Shi-Yao(林士耀)[a)], and Kong Wei(孔 伟)[a)]

[a)] *Institute of Plasma Physics, Chinese Academy of Science, Hefei* 230031, *China*

[b)] *Institute of Electronic Engineering, Hefei* 230037, *China*

(Received 1 July 2005; revised manuscript received 26 August 2005)

Multi-channel soft x-ray (SX) detectors are applied to generate images of magnetohydrodynamic (MHD) oscillation on the HT-7 tokamak, and the data from SX cameras are analysed by using the Fourier–Bessel harmonic reconstruction method and the singular value decomposition. The image reconstruction of SX emissivity is obtained on the assumption of plasma rigid rotation. One of the important phenomena in the HT-7 discharge is the transition from the sawtooth oscillations to the MHD oscillations when the plasma density grows higher. The MHD structure observed in the SX tomography is featured as follows: the magnetic surface of MHD structure is made up of the crescent-shaped "hot core" and the circular "cold bubble". The structure of the magnetic surface is relatively stable. It rotates in the direction of the electron diamagnetic drift at a frequency being the oscillation frequency of the MHD oscillations.

Keywords: soft x-ray tomography, magnetohydrodynamic oscillation, singular value decomposition
PACC: 5270, 5270L

1. Introduction

Magnetohydrodynamic (MHD) instabilities are the prevalent and important phenomena in tokamaks. They are responsible for lowering energy confinement and limiting the achievable beta values in tokamaks. Moreover, they can cause major disruptions in the plasma to destroy the plasma.[1−4] Therefore, in order to obtain a high confinement and high beta plasma, it is very important to investigate the mechanism of the MHD instabilities. Various diagnostics have been developed to study perturbations caused by the MHD instabilities in fusion plasmas. The soft x-ray tomography diagnostics[5,6] plays a key role in the study of MHD instabilities, since the two-dimensional (2D) images allow the detailed study of the spatial structure of the instabilities. Another important diagnostic system of investigating the MHD instabilities is a grating polychromator system,[7] which measures electron temperature perturbations by detecting the electron cyclotron emission. Recently, the singular value decomposition (SVD), a new tool of spectrum analysis for multi-channel diagnostic systems, has been applied to Mirnov coil signals to identify the mode numbers of MHD instability[8,9] and to SX signals to investigate the structure of MHD instability.[10−13] Additionally, the technique can be used to improve the signal-to-noise ratio by omitting the terms of small singular values.

In this paper, we present the SX tomography of the MHD oscillations to better study the characteristics of the MHD structure by using SX multi-channel diode arrays. And we use the SVD technique to analyse the structure and the mode numbers of the MHD oscillations. Furthermore, we also employ the SVD technique to improve the signal-to-noise ratio with a special filtering of rapid time evolution. After a brief description of the SX system of the HT-7 tokamak in

*Project Supported by the National Natural Science Foundation of China (Grant Nos 10375070 and 10305012).
†E-mail: tpma@ipp.ac.cn

Section 2, the experimental results are presented in Section 3. The discussion is given in Section 4, and conclusion in Section 5.

2. Experimental apparatus

HT-7 tokamak has major and minor radii of R_0=122cm and a=27cm, respectively.[14] The SX diagnostic system, shown in Fig.1, consists of two imaging cameras with slot-apertures, which horizontally and vertically view a given toroidal cross-section of the plasma from different poloidal chords, each camera containing 37 Au-Si surface-barrier diode detectors.[15–17] All detectors are mounted on the arc-shaped stainless-steel pedestals with R=55cm in horizontal array and R=60cm in vertical array. Their spatial resolution, the radial distance between neighbouring viewing chords of the detectors, is 1.5cm. They view the plasma from –27cm to 27cm along the given chords through thin slot-apertures with an area of $5\times20\text{mm}^2$ in the vertical array and $4\times25\text{mm}^2$ in the horizontal array. The time resolution ranges from about 4μs to 12.8μs. The spatial profile of the SX emissivity is reconstructed by computer tomography based on the Fourier–Bessel expansion technique,[18] which is suited to describing the circular plasma cross section in HT-7 tokamak.

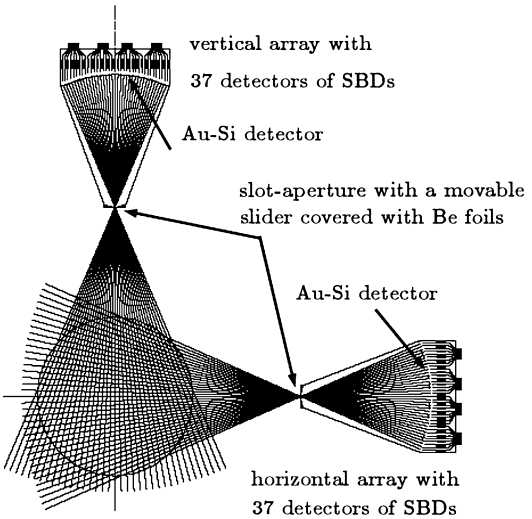


Fig.1. The SX imaging system on the HT-7 tokamak.

3. Experimental results

We have observed the MHD oscillations on the intensity signals of the SX in the lower hybrid wave (LHW) and ion Bernstein wave (IBW) synergetic discharges with the following plasma parameters: plasma current I_p ≈122 kA, central chord-averaged electron density $N_\text{e}(0)\approx1.97\times10^{13}\,\text{cm}^{-3}$, a toroidal magnetic field $B_\text{t}(0)\approx1.82$T at the plasma centre, P_LHW ≈250 kW and P_IBW ≈155 kW. The discharge waveforms of Shot 54936 are shown in Fig.2.

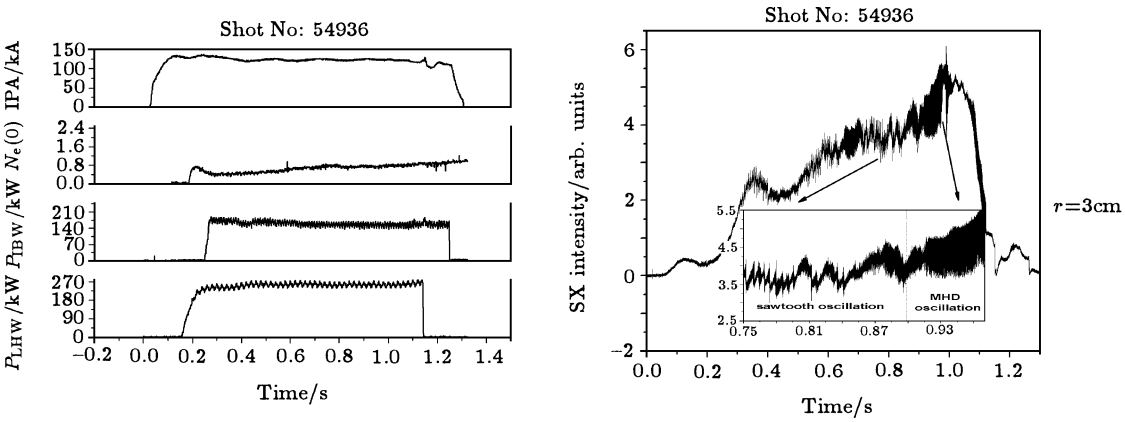


Fig.2. The discharge waveforms of Shot 54936.

When the LHW and IBW are applied, the intensity of SX rises and the sawtooth period increases gradually. Eventually, the sawtooth oscillations transits to the MHD oscillations at about 900ms. The profile of electron density derived from the Abel inversion is shown in Fig.3. It is very clear that $n_e(r)$ grows higher and its spatial profile becomes more and more peaked during LHW and IBW synergetic heating. Variations of the electron density roughly reflect the changes of the pressure. Hence, it seems that the pressure-gradient in the central area grows steep, and the characteristics of the central MHD activities are strongly affected. The MHD oscillations on the SX signals near the centre for Shot 54936 are shown in Fig.4.

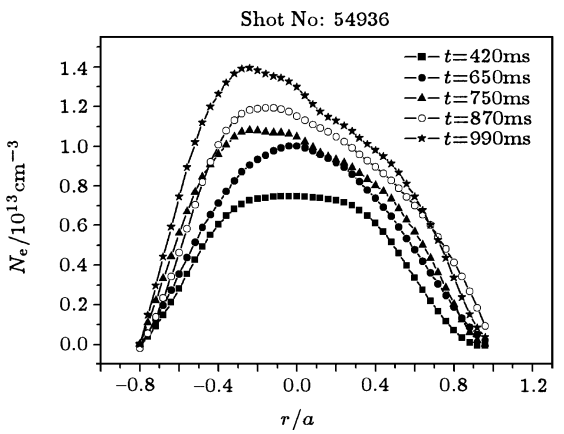


Fig.3. The electron density profiles for Shot 54936.

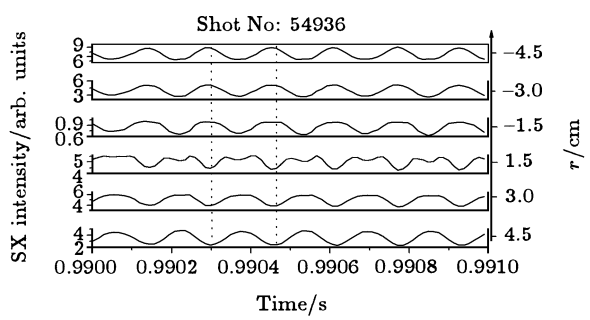


Fig.4. The SX signals near the centre of the (1,1) MHD-mode oscillations for Shot 54936.

The contour plots of SX signals shown in Fig.5 reflect the even stronger MHD activity. The temporal evolution and spatial localization of the m=1, n=1 ((1,1)) mode are clearly visualized, where m and n are the poloidal and toroidal mode numbers. The letters P and N denote the positive and negative perturbations respectively in the figure. Phase inversion at $r/a \sim 0.3$, which is one of the distinctive features of the (1,1) mode, is also revealed.

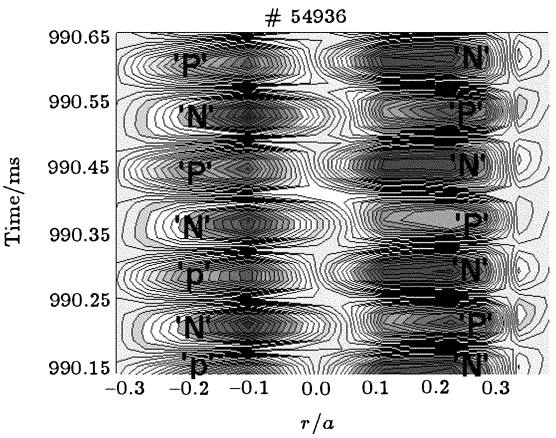


Fig.5. Contour plot SX signals reflecting the (1,1) MHD-mode activity.

Using the SVD analysis, we have obtained the temporal and the spatial structures of this mode. Figure 6 shows the results of the SVD analysis. The first temporal eigenvector gives the evolution of the equilibrium emission, and its spatial eigenvector reflects the spatial distribution of SX emission. It is clear that the (1,1) MHD perturbation is described by the second eigenvector. The temporal eigenvector reflects the repetition time about 0.18ms, as shown in Fig.6 (a), while the spatial eigenvectors point to the characteristic radius r_1 ≈3.73cm, as shown in Fig.6(b). The spectrum in singular values from 1 to 37 is shown in Fig.6(c). The first two eigenvalues, whose quality of filtering is $\Delta_2 \approx 0.9913$, which reveals approximately two significant components containing almost all of the signal energies. Therefore, in order to improve the signal-to-noise ratio by omitting the terms of small singular values, we choose the first two terms as the spatial-temporal signals in this paper. The contribution of the other terms to the total signal is small, or noisy.

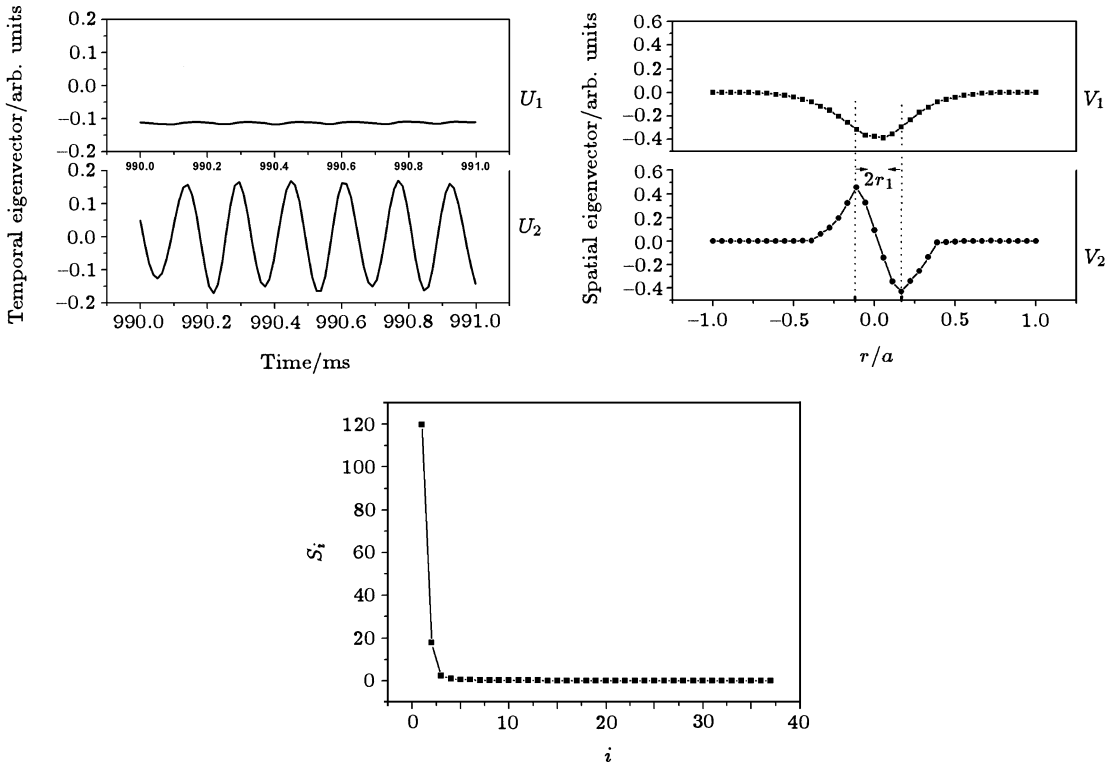
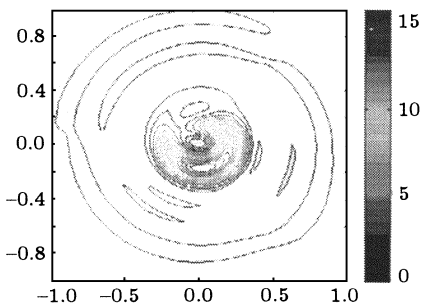
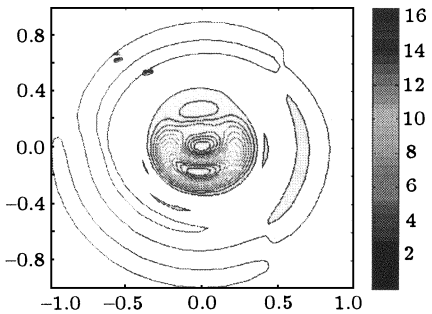


Fig.6. The results of the SVD analysis. (a) is for the first two temporal eigenvectors of the discharge #54936. The first temporal eigenvector U_1 gives the evolution of the equilibrium emission. The second temporal eigenvector U_2 indicates the evolution of the (1,1) MHD oscillation. (b) is for the first two spatial eigenvectors of the discharge #54936. The first spatial eigenvector V_1 reflects the spatial distribution of SX emission. The second eigenvector V_2 shows the spatial structure of the (1,1) MHD-mode activity. (c) is for spectrum of the singular values from 1 to 37.

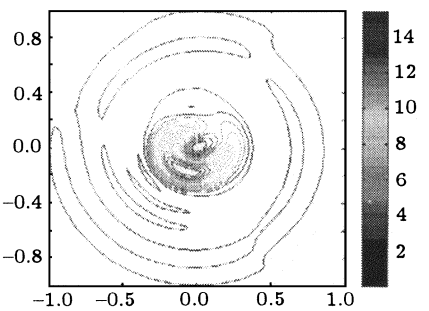
Because the amplitude of the (1,1) MHD-mode does not change significantly (Fig.4), we take only one period of these oscillations into account. The contour maps of the SX emissivity in one period of the (1,1) MHD-mode oscillations (from 990.304ms to 990.460ms) are shown in Fig.7. From the 2D image reconstruction of SX emissivity, we can conclude that the characteristics of the (1,1) MHD-mode structure as follows: the magnetic surface of (1,1) MHD-mode structure is made up of the crescent-shaped "hot core" and the circular "cold bubble". The "hot core" does not stay in the central region of the plasma, but moves outward to the vicinity of the q=1 surface. The circular "cold bubble" is located at the opposite of the hot core. The structure of the magnetic surface is relatively stable. It rotates in the direction of the electron diamagnetic drift at a frequency being the oscillation frequency of the (1,1) MHD-mode.



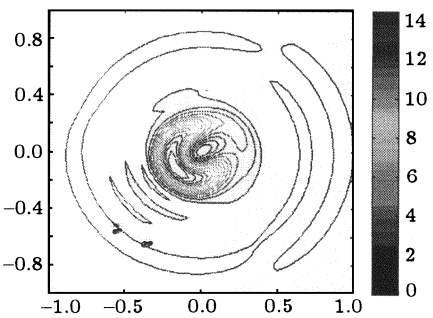
t=990.304ms



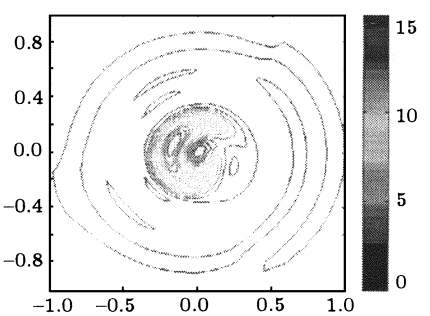
t=990.317ms



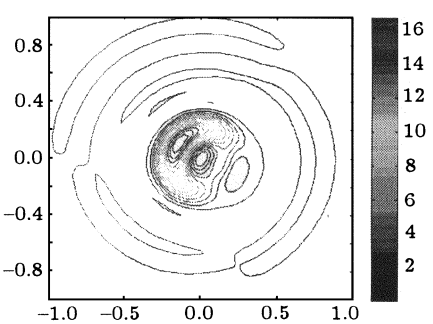
t=990.330ms



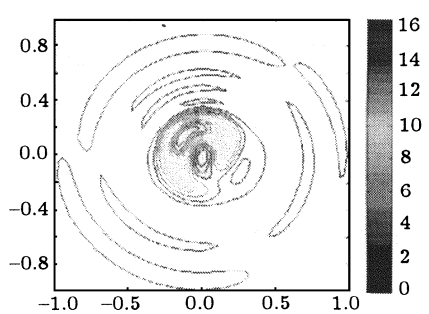
t=990.343ms



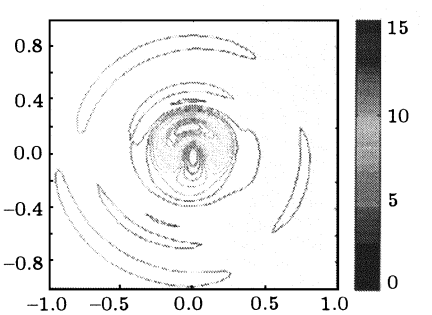
t=990.356ms



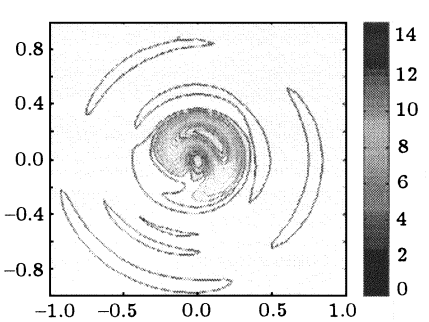
t=990.369ms



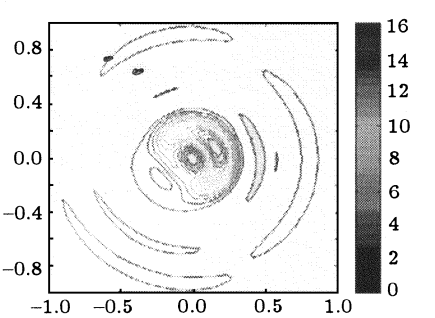
t=990.382ms



t=990.395ms



t=990.408ms



t=990.421ms

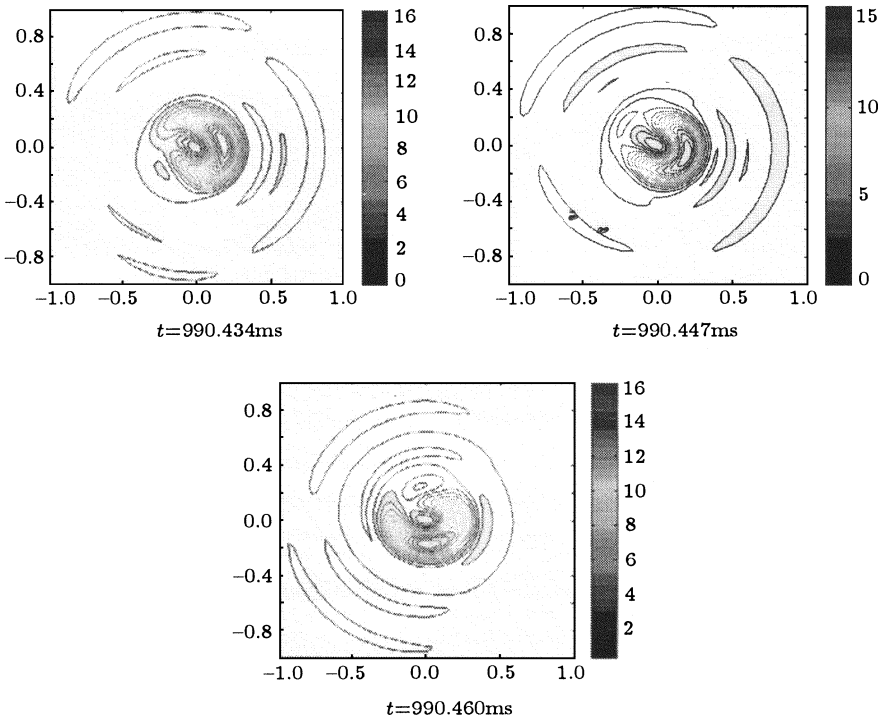


Fig.7. The contour plots of the emissivity maps in one period of the (1,1) MHD oscillations.

4. Discussion

From Fig.7 above, the whole magnetic surface is relatively stable. Which could be understood as follows: the stable configuration is maintained by the stable bubble with a second magnetic axis and a high rotation speed.

As described in Ref.[19], the authors pointed out that artefacts appeared in SX images based on the Fourier–Bessel expansion technique when the angular mode numbers used for computer tomography imaging were not sufficient. Especially, an off-centred circular hot core pushed at the inversion radius in the case of Kadomtsev type of crash looks like a crescent shape if numbers used for the angular expansion are restricted to m=0 and 1. Angular mode numbers up to m=3 are sufficient to distinguish the crescent shape from the circular shape.[20,21] Therefore, in all the SX images in this paper, mode numbers up to m=4 and l=7 have been used for the angular and radial expansions, respectively, which are determined with the help of the Akaike information criterion.[22] Furthermore, in this paper, all the data are measured by the horizontal array; the plasma rigid rotation is assumed.

5. Conclusion

We have obtained tomographic reconstructions of the SX emissivity on the assumption of plasma rigid rotation, and applied the pre-processing and post-processing SVD technique, which is a powerful tool well suited to the study of spatial-temporal signals, to the tomography reconstructed image in order to obtain clearer profile. One of the important phenomena in the HT-7 discharge is the transition from the sawtooth oscillations to the MHD oscillations when the plasma density goes higher. The MHD structure observed in the SX tomography is featured as follows: the magnetic surface of MHD structure is made up of the crescent-shaped "hot core" and the circular "cold bubble". The structure of the magnetic surface is relatively stable. It rotates in the direction of the electron diamagnetic drift at a frequency being the oscillation frequency of SX signals.

Acknowledgement

The authors would like to thank Professor Yi Liu of the South-Western Institute of Physics, Chengdu, China for valuable discussions.

References

[1] Chang Z, Fredrickson E D, Callen J D, Mcguire K M, Bell M G, Budny R V, Bush C E, Darrow D S, Janos A C, Johnson L C, Park H K, Scott S D, Strachan J D, Synakowski E J, Taylor G, Wieland R M, Zarnstortt M C, Zweben S J and TFTR Team 1994 *Nucl. Fusion* **34** 1309

[2] Snipes J A, Campbell D J, Hender T C, Von Hellermann M and Weisen H 1990 *Nucl. Fusion* **30** 205

[3] Yu C X, Brower D L, Zhao S J, Bravenec R V, Chen J Y, Lin H, Luhmann N C, Jr, Peebles W A , Ritz C P, Schoch P M and Yang X Z 1992 *Nucl. Fusion* **32** 1545

[4] Wesson J A, Gill R D, Hugon M, Schuller F C, Snipes J A, Ward D J, Bartlett D V, Campbell D J, Duperrex P A, Edwards A W, GRanetz R S, Gottardi N A O, Hender T C, Lazzaro E, Lomas P J, Lopes Cardozo N, Mast K F, Nave M F F, Salmon N A, Smeulders P, Thomas P R, Tubbing B J D, Turner M F and Weller A 1989 *Nucl. Fusion* **29** 641

[5] Granetz R S and Smeulders P 1988 *Nucl. Fusion* **28** 457

[6] Cruz da D F, Jr and Donne A J H 1994 *Rev. Sci. Instrum* **65** 2295

[7] Ishida S, Nogashima A, Sato M, Isei N and Matoba T 1990 *Rev. Sci. Instrum* **61** 2834

[8] Nardine C 1992 *Plasma Phys. Control. Fusion* **34** 1447

[9] Kim J S, Edgell D H, Greene J M, Strait E J and Chance M S 1999 *Plasma Phys. Control. Fusion* **41** 1399

[10] Marrelli L, Bilato R, Franz P, Martin P, Murari A and O'Gorman M 2001 *Rev. Sci. Instrum* **72** 499

[11] Dudok de Wit T, Pecquet A L, Vallet J C and Lima R 1994 *Phys. Plasmas* **1** 3288

[12] Dudok de Witt T 1995 *Plasma Phys. Control. Fusion* **37** 117

[13] Anton M, Weisen H, Dutch M J, von der Linden W, Buhlmann F, Chavan R, Marletaz B, Marmillod P and Paris P 1996 *Plasma Phys. Control. Fusion* **38** 1849

[14] Shi Y J, Wan B N, Chen Z Y, Hu L Q, Lin S Y, Ruan H L, Qian J P, Zhen X J, Ding B J, Kuang G L, Li J G and HT-7 Team 2005 *Chin. Phys.* **14** 1193

[15] Ma T P, Hu L Q, Wan B N, Ruan H L, Gao X, Zhen X J, Zhou L W, Sun Y W, Chen Z Y, Lin S Y and Kong W 2005 *Chin. Phys.* **14** 2061

[16] Hu L Q, Wei M S, Ling B L, Fang Z S and Zeng L 2000 *Plasma Sci. Technol.* **2** 515

[17] Hu L Q, Wan B N, Shi Y J, Yang Y, Gao X, Li J G, Kuang G L, Zhao Y P, Xie J K, Mao J S and Xu Y 2003 *Plasma Phys. Control. Fusion* **45** 349

[18] Nagayama Y 1987 *J. Appl. Phys* **62** 2702

[19] Janicki C, Decoste R and Simm C 1989 *Phys. Rev. Lett* **62** 3038

[20] Kadomtsev B B 1975 *Sov. J. Plasma Phys.* **1** 389

[21] Wesson J A 1986 *Plasma Phys. Control. Fusion* **28** 243

[22] Akaike H 1974 *IEEE Trans. Autom. Control* **AC-19** 78